# Characterization of Amyloid Formation by Glucagon-Like Peptides: Role of Basic Residues in Heparin-Mediated Aggregation

Narendra Nath Jha,[†] A. Anoop,[†] Srivastav Ranganathan, Ganesh M. Mohite, Ranjith Padinhateeri, and Samir K. Maji*

Department of Biosciences and Bioengineering, IIT Bombay, Mumbai 400 076, India

S *Supporting Information*

ABSTRACT: Glycosaminoglycans (GAGs) have been reported to play a significant role in amyloid formation of a wide range of proteins/peptides either associated with diseases or native biological functions. The exact mechanism by which GAGs influence amyloid formation is not clearly understood. Here, we studied two closely related peptides, glucagon-like peptide 1 (GLP1) and glucagon-like peptide 2 (GLP2), for their amyloid formation in the presence and absence of the representative GAG heparin using various biophysical and computational approaches. We show that the aggregation and amyloid formation by these peptides follow distinct mechanisms: GLP1 follows nucleation-dependent aggregation, whereas GLP2 forms amyloids without any significant lag time. Investigating the role of heparin, we also found that heparin interacts with GLP1, accelerates its aggregation, and gets incorporated within its amyloid fibrils. In contrast, heparin neither affects the aggregation kinetics of GLP2 nor gets embedded within its fibrils. Furthermore, we found that heparin preferentially influences the stability of the GLP1 fibrils over GLP2 fibrils. To understand the specific nature of the interaction of heparin with GLP1 and GLP2, we performed all-atom MD simulations. Our in silico results show that the basic-nonbasic-basic (B-X-B) motif of GLP1 (K28-G29-R30) facilitates the interaction between heparin and peptide monomers. However, the absence of such a motif in GLP2 could be the reason for a significantly lower strength of interaction between GLP2 and heparin. Our study not only helps to understand the role of heparin in inducing protein aggregation but also provides insight into the nature of heparin–protein interaction.

Interaction of GLP1 with heparin
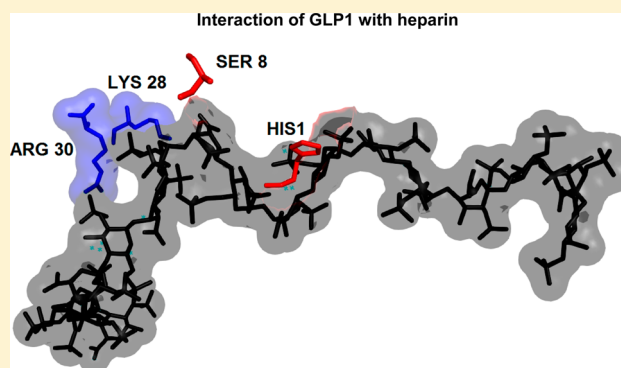
A myloids are highly ordered cross-β-sheet-rich protein/peptide aggregates that are historically associated with neurodegenerative diseases such as Alzheimer's and Parkinson's.[1] Recent evidences have suggested that amyloids are not only associated with diseases but also can perform native functions in the host organism. Amyloids associated with normal biological functions are called functional amyloids. Examples of functional amyloids include Curli in *Escherichia coli*, Chaplin in fungi, and yeast prions.[2] Two mammalian functional amyloids discovered recently were pMel17 amyloid in melanosomes and protein/peptide hormone amyloids within the secretory granules of the pituitary gland.[3,4] It has been suggested that the secretion of protein/peptide hormones in regulated secretory pathways involves aggregation and condensation of the protein/peptide into membrane-enclosed secretory granules.[5−8] However, the nature of the aggregates inside the secretory granules was not known. Recently, it was suggested that peptides/proteins formed an amyloid-like structure inside the secretory granules that can release functional protein/peptide upon secretion into the extracellular space.[4]

The secretory proteins of regulated pathway in cells have been reported to aggregate at the trans-golgi network before packaging into the secretory granules.[5−7,9] Several factors, including pH, ionic strength, and copackaging proteins, play an important role in this event.[10−13] More importantly, the existence of certain inducer molecules like glycosaminoglycans (GAGs) at this compartment of the cell plays a pivotal role in the aggregation and subsequent granule packaging/condensation of the cargo.[4,13−16] Glycosaminoglycans have also been observed along with disease-related amyloid deposits in organs, and many studies have shown that these promote fibrillation of several amyloidosis-associated proteins.[17−24] The specific mechanism by which heparin induces amyloid formation is, however, not clearly understood. Deciphering the nature of heparin–peptide interactions would be crucial to understand the manner in which GAGs facilitate peptide/protein hormone aggregation during their packaging and storage. Several studies have reported that the availability of basic amino acid residues in the protein/peptide favors interaction with glycosaminoglycans. Moreover, XBBBXXBX or XBBXBX sequences were suggested and experimentally proved to be the consensus

heparin-binding domains, where B is a basic amino acid and X is a nonbasic amino acid.[25−28]

In the present work, we selected two closely related peptides, glucagon-like peptide 1 and 2 (GLP1 and GLP2), which have previously been shown to form amyloid-like structures in vitro in the presence or absence of the glycosaminoglycan heparin.[4] Previously, glucagon, a closely related peptide hormone, has also been reported to form amyloid-like structures and to display polymorphism in its fibril morphology at different concentrations[29−31] and in the presence of additives like sulfate ions.[32] Additionally, it was suggested that these hormones could be stored as amyloids within the secretory granules.[4] GLP1 and GLP2 are generated from a common precursor proglucagon (180 amino acid residues) from the regions comprising amino acid residues 72−108 and 126−158, respectively.[33] Both of these peptides have been shown to be stored inside the secretory granules of the pancreatic α-cells and intestinal L-cells.[34] The amino acid sequences of these two peptides are highly similar (80%) and also exhibit 37% identity (Figure 1A,B). Here, we focus on understanding the aggregation

Figure 1. Sequence homology in GLP1 and GLP2 (A) showing residues that are conserved between GLP1 and GLP2 and (B) indicating the location of the conserved residues in the 3D structure of the two peptides, GLP1 (PDB ID 1D0R, left) and GLP2 (PDB ID 2L63, right).

behavior of GLP1 and GLP2 (in the presence or absence of heparin), and we probe whether their sequence similarity imparts a commonality to their self-assembly process. Furthermore, this study was aimed to elucidate whether a small level of sequence variation could significantly change the nature of the interaction with the glycosaminoglycan heparin. Studying the detailed mechanism of GLP1 and GLP2 amyloid formation is thus important to understand the aggregation of proteins/peptides targeted to secretory granules in mammalian cells.

In the current study, we observed a large structural transition in GLPs during the process of amyloid fibril formation using biophysical techniques. We found that heparin preferentially interacts and accelerates fibril formation in GLP1; however, it

does not play a significant role in GLP2 amyloid formation. Heparin was incorporated into GLP1 fibrils and it stabilized them against monomer release, whereas minimal involvement of heparin was observed in the case of GLP2. All-atom molecular dynamics simulations using NAMD[35] were also performed to study the probable role of heparin in the aggregation of GLP1 and GLP2. Consistent with our in vitro data, the MD simulations also revealed the preferential binding of heparin to GLP1 over GLP2. We propose that the reason for this favored heparin interaction is possibly due to the availability of a higher number of basic amino acid residues and the presence of a single basic-nonbasic-basic (B-X-B) sequence in GLP1. Our findings will not only significantly augment the existing knowledge on the role of GAGs in peptide/protein hormone aggregation and storage as amyloids inside secretory granules but also highlight the mechanism of amyloid formation of proteins/peptides associated with diseases.

■ MATERIALS AND METHODS

Chemicals and Reagents. The peptides GLP1 and GLP2 were purchased from BACHEM (Bubendorf, Switzerland). Other chemicals and reagents used for the study were purchased from Sigma-Aldrich (Steinheim, Germany) and Calbiochem (San Diego, CA, USA). Double-distilled and deionized water for the study was used from a TKA Lab Tower AFT (Niederelbert, Germany).

In Vitro Aggregation of GLPs. Peptides were dissolved in 500 μL of 5% D-mannitol containing 0.01% sodium azide (v/v) at a concentration of 1 mg/mL. GLP1 dissolved completely, resulting in a clear solution, but GLP2 was not completely soluble. To solubilize GLP2, 0.1 N NaOH was added dropwise until the solution became clear; the pH of the resultant solution was close to 9.0. The pH was then adjusted to 5.8 by the dropwise addition of 0.1 N HCl. Both GLP1 and GLP2, adjusted to pH 5.8 (secretory granule relevant pH), were ultracentrifuged at 90 000 rpm for 45 min, and the supernatant was used for aggregation studies. The concentrations of GLPs were determined by absorbance at 280 nm using molar absorptivities (ε) of 6990 M^{-1} cm^{-1} for GLP1 and 5500 M^{-1} cm^{-1} for GLP2. To check the 'seed-free' nature of the peptide solutions (supernatant after ultracentrifugation), electron microscopy (EM) was performed.

For aggregation experiments, 250 μL each of GLP1 and GLP2 (~150 μM) was aliquoted into four separate low-binding microfuge tubes (Eppendorf AG, Hamburg, Germany), and an equimolar concentration of heparin was added to one tube each of GLP1 and GLP2. The samples (stocks) were incubated at 37 °C, and circular dichroism (CD) thioflavin T (ThT) fluorescence studies were carried out at regular intervals to determine the aggregation kinetics. All experiments were repeated three times.

Circular Dichroism Spectroscopy (CD). Far-UV CD was used to monitor the secondary structure of GLPs during the aggregation studies. For CD, aliquots of each sample from stock were diluted with 5% D-mannitol containing sodium azide (0.01%) such that the final peptide concentration was ~20 μM. Diluted samples were transferred into a 0.1 cm path length quartz cell (Hellma, Forest Hills, NY), and spectra were acquired using a JASCO 810 CD instrument. All measurements were performed at 25 °C from 198 to 260 nm. Raw data were processed by smoothing (Savitzky−Golay procedure) and buffer spectra subtraction.
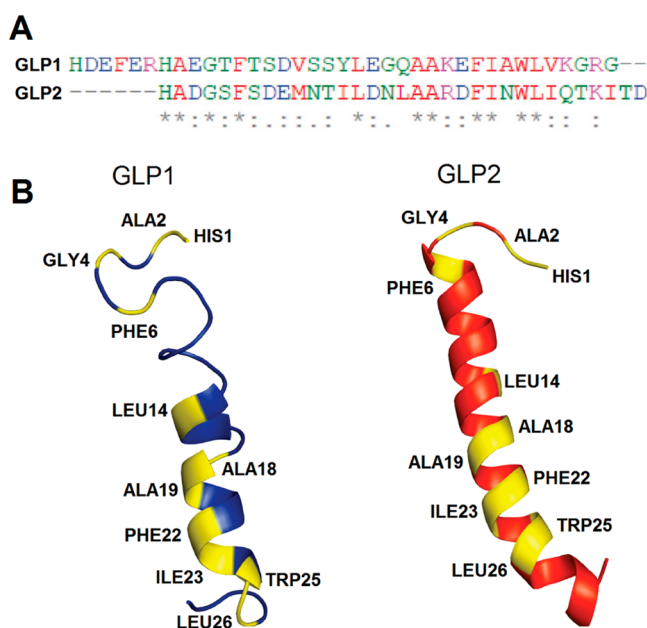
Thioflavin T Fluorescence. The kinetics of fibril formation was monitored by the increase in fluorescence of amyloid-specific dye thioflavin T (ThT). An aliquot of peptide sample was diluted to 500 μL in 5% D-mannitol containing 0.01% (w/v) sodium azide such that the final peptide concentration was ~10 μM. Two microliters of 1 mM ThT was added into 200 μL of diluted sample, which was then mixed immediately in a 1 cm path length quartz microcuvette (Hellma, Forest Hills, NY), and the ThT fluorescence was measured using a spectrofluorimeter (Hitachi F-2500) by exciting the samples at 450 nm and recording the emission spectra in the range of 460−500 nm. The excitation and emission slit widths were kept at 5 nm. The emission values at 482 nm were plotted against incubation time.

Using the fluorescence data as the basis, the lag times (t_{lag}) for GLP amyloid formation were calculated using eqs 1 and 2, where y is the intensity of ThT fluorescence.[36]

$$ y = y_0 + \frac{(y_{max} - y_0)}{(1 + e^{-k(t-t_{1/2})})} \tag{1} $$

$$ t_{lag} = t_{1/2} - \frac{2}{k} \tag{2} $$

ANS (8-Anilinonaphthalene-1-sulfonate) Fluorescence. For the ANS fluorescence study, aliquots of the incubated peptide solutions were diluted to 200 μL such that the final peptide concentration was ~10 μM. The solution was taken into a 1 cm path length quartz cuvette, and 2 μL of 5 mM ANS was added to this followed by a 5 min incubation in dark. The ANS fluorescence spectra were recorded using a spectrofluorimeter (Hitachi F-2500), with an excitation wavelength of 370 nm and emission wavelength ranging from 400 to 600 nm. The excitation and emission slit widths were kept at 5 nm. The ANS fluorescence at 490 nm was plotted against incubation time.

Tryptophan (Trp) Fluorescence and Acrylamide Quenching. An aliquot of peptide samples was diluted to 500 μL in 5% D-mannitol containing 0.01% (w/v) sodium azide such that the final peptide concentration was ~10 μM. The Trp fluorescence was measured in a rectangular 10 mm quartz microcuvette using a spectrofluorimeter (Hitachi F-2500), with excitation at 280 nm and emission ranging from 290 to 500 nm. The excitation and emission slit widths were kept at 2.5 nm. For the acrylamide quenching experiment, 200 μL of the diluted stock was taken in a 1 cm path length quartz cuvette, acrylamide was added to a final concentration of 0, 50, 100, 150, 200, 250, 300, 350, and 400 mM, and Trp fluorescence was recorded as mentioned above. The fluorescence intensity at each concentration of acrylamide was corrected by the dilution factor of the added volume of acrylamide. The maximum fluorescence intensity in the absence of acrylamide was considered as F_0, and the maximum fluorescence intensity in the presence of different concentrations of acrylamide, as F. The ratio F_0/F was calculated and plotted against concentrations of acrylamide [Q]. As the plots deviated from linearity (because of both static and dynamic quenching), we used a modified Stern−Volmer equation to calculate the quenching constant

$$ F_0/F = (1 + K[Q]) e^{V(Q)} $$

where K is the dynamic quenching constant and V is the static quenching constant.

Dot-Blot Analysis. GLP1 and GLP2 fibrils formed in the presence of heparin were used for dot-blot analysis. Equal amounts of samples (5 μL each) from the aggregation stock were spotted on a nitrocellulose membrane (Immobilon-NC, Millipore) and allowed to air-dry for 8 min. Two washes (2 × 8 min) were performed with PBST (137 mM NaCl, 2.7 mM KCl, 10 mM Na_2HPO_4, 2 mM KH_2PO_4, and 0.1% Tween), and the membrane was blocked with 5% nonfat milk powder (Himedia, Mumbai, India) in PBST for 1 h at room temperature. The blot was incubated with anti-heparin antibody (1:200 dilution, MAB2040, Chemicon) overnight at 4 °C followed by PBST washes, and the blot was then incubated with horseradish peroxidase-conjugated secondary antibody (1:1000 dilution, cat. no. 401253, Calbiochem). After this step, three washes were performed with TBST (50 mM Tris, 150 mM NaCl, and 0.1% Tween), and the blot was developed after it was exposed to chemiluminescent substrate (SuperSignal West Pico, Pierce).

Monomer Release Assay. Amyloid fibrils of GLP1 and GLP2 (100 μL of 100 μM each) were subjected to dialysis through a 10 kDa cutoff membrane against 500 μL of 5% D-mannitol containing sodium azide (0.01%). The Slide-A-Lyzer mini dialysis unit system (Pierce, Rockford, IL, USA) was used for this study. The mini dialysis units containing samples were capped and placed into a 1 mL Nunc cryo tube (Nunc, Denmark) having 500 μL of 5% D-mannitol with sodium azide (0.01%). Small magnetic bars were placed into individual tubes, and the assembled units were placed on a magnetic stirrer (Spinot, Jaibro Scientific Works, New Delhi, India). After suitable time intervals, the solution from outside the dialysis membrane was taken for analysis. To monitor the monomer release, an aliquot of 150 μL of the solutions from the cryo tube (outside the membrane) was taken, and tryptophan fluorescence was measured. The fluorescence readings were taken at time points 0, 6, 12, and 24 h. Following the recording of each spectra, the outside solution was returned, and the dialysis system was reassembled as described above. Experiments were repeated twice.

Transmission Electron Microscopy. Ten microliters of ~40 μM incubated samples (30 days old) of GLP1 and GLP2 were spotted on a carbon-coated Formvar grid (Electron Microscopy Sciences, Fort Washington, PA, USA) and incubated for 5 min at room temperature. The samples were washed twice with autoclaved distilled water, and the remaining water was wiped gently with filter paper. The samples were then stained with 10 μL of 1% (w/v) aqueous uranyl formate solution for 5 min followed by air-drying. The images were taken at magnifications 26 000× and 43 000× at 120 kV using a transmission electron microscope (TECNAI12 D312 FEI, The Netherlands). Experiments were repeated twice with two independent samples.

MD Simulation. The intermolecular interactions (interpeptide and peptide-heparin) driving peptide aggregation were studied at atomistic details using molecular dynamics (MD) simulations. The starting structures for the GLP1 and GLP2 simulations were obtained from PDB IDs 1D0R and 2L63, respectively. The two peptides were first energy-minimized in vacuum using 2000 steps of the conjugate-gradient (CG) algorithm. The energy-minimized structures were then solvated in TIP3P water, and the solvated system was further energy-minimized for another 15 000 steps of the CG algorithm. The solvated system was then charge-neutralized using Na^+ and Cl^- ions and further energy-minimized for 1500 steps. The completely solvated and charge-neutralized system was then
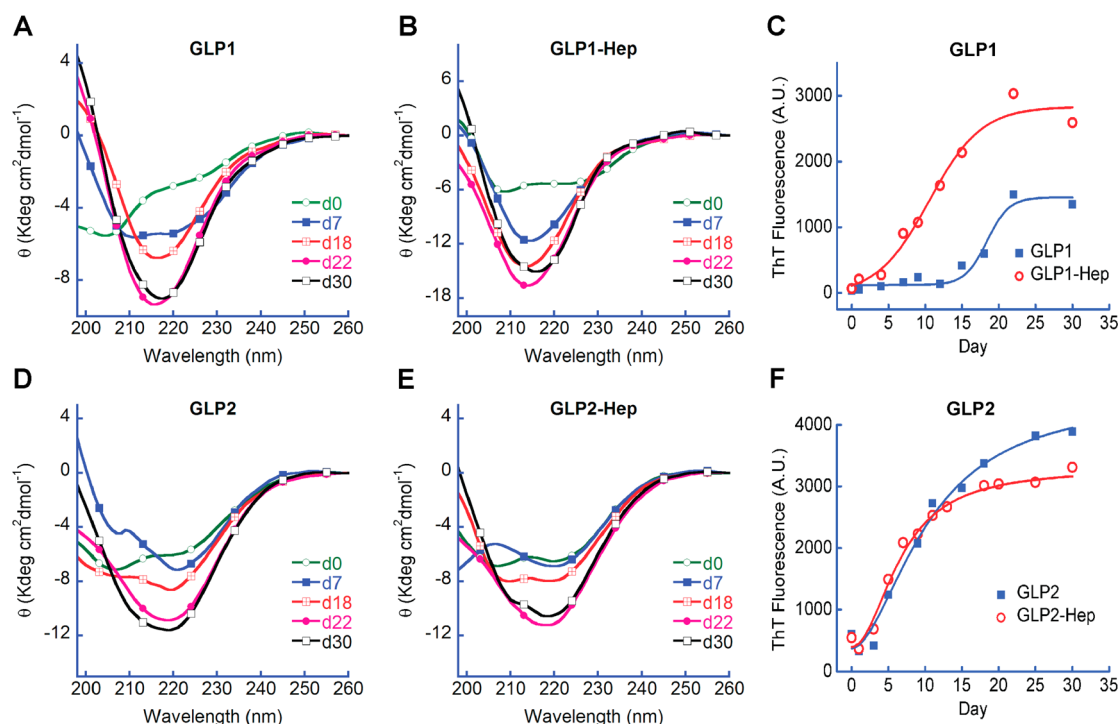
Figure 2. Secondary-structure changes and kinetics of GLP amyloid formation. CD spectra of (A) GLP1 without heparin (GLP1) show a slower rate of secondary-structural transformation when compared to (B) GLP1 with heparin (GLP1-Hep). (D) GLP2 without (GLP2) and (E) with heparin (GLP2-Hep) show similar secondary-structure transitions with time. ThT fluorescence as a function of incubation time indicates that GLP1 follows sigmoidal kinetics during fibril formation, displaying an initial lag time and then elongation followed by a stationary phase (C), whereas GLP2 does not show any significant lag time. We observed similar kinetics for GLP2 in the presence and absence of heparin (F). The spectra were recorded at the times indicated in the figure, where d indicates day.

subjected to linearly scaled heating (0.001 K/step) for 310 000 steps; gradually heating the system from 0 to 310 K. The thermalized system was then equilibrated for another 1 ns under NPT (constant temperature and pressure) conditions and finally used for the production run of 100 ns each. All simulations were performed under NPT conditions with an electrostatic cutoff distance of 12 Å units and a van der Waals cutoff of 10 Å units. The MD package NAMD 2.9 was used for simulating the systems. The two systems used for simulation consisted of eight peptides in presence of one heparin molecule in explicit TIP3P water such that no biased interactions exist initially. The heparin (pentasaccharide) structure was obtained from the anti-thrombin pentasaccharide complex in the PDB (PDB ID 1AZX). The snapshots from the simulation were rendered using PyMol[37] and Chimera,[38] and the interaction map was plotted using LigPlot.[39]

■ RESULTS

Amyloid Fibril Formation by GLP1 and GLP2. To study the fibril formation by GLP1 and GLP2, peptides were dissolved in 5% D-mannitol and 0.01% sodium azide, and seed-free solutions were prepared using ultracentrifugation. Peptides were incubated at 37 °C, and amyloid formation was monitored at regular time intervals by ThT binding, CD spectropolarimetry, and EM studies. The amyloid-specific dye ThT binds to the cross-β-sheet structure of amyloids[40] and therefore it is used to monitor the kinetics of amyloid formation by peptide/proteins.[41] Amyloid formation requires the protein/peptide to pass through a nucleation event to form higher-order structures. This transition of peptides/proteins from a monomeric state to an amyloid state is considered to be an

energy-barrier-dependent process in which the free-energy maxima corresponds to the formation of fibril nucleus.[42] Sigmoidal growth kinetics (curve) for amyloid formation can be obtained by recording ThT fluorescence at different time points during aggregation.[43] The initial lag time in the curve corresponds to low ThT binding with insignificant ThT-positive fibrils in the solution.[44] After the initial lag time, the log phase (amyloid growth phase) begins, indicated by a rapid increase in ThT binding, which becomes stationary once the amyloid fibril formation is completed.[43,45]

In the present study, GLP1, both in the presence and absence of heparin, showed an increase in ThT fluorescence with time; however, this increase was more significant in the case of GLP1-Hep than GLP1 alone (Figure 2C). GLP2 also showed an increase in ThT fluorescence with time, but there was no significant difference in the presence or absence of heparin (Figure 2F). A deviation in the ThT fluorescence profile for GLP2 and GLP2-Hep observed beyond 10 days (Figure 2F) could be the result of partial precipitation and/or higher-order association of GLP2 filaments in the presence of heparin. We observed nucleation-dependent amyloid formation by GLP1 in the presence and absence of heparin. The sigmoid curves of the time-dependent change in ThT fluorescence show a shorter lag time (~5 days) in the case of GLP1 in the presence of heparin as compared to GLP1 alone (~13 days), indicating the role of heparin in accelerating fibrillation. This was followed by an exponential growth phase and a stationary phase (Figure 2C). In presence of heparin, GLP2 did not show any marked difference in kinetics compared to that in the absence of heparin, suggesting that heparin might not be actively involved in fibril formation by GLP2. In the presence

and absence of heparin, GLP2 showed both log and stationary phases with a very short lag time (GLP2, 3 days; GLP2-Hep, ~2.5 days) (Figure 2F), which indicates that relatively rapid fibrillation/aggregation has possibly taken place in both of these cases. It is possible that higher-order oligomers have formed immediately after dissolution of this peptide both in the presence and in absence of heparin.

To test whether the differences in GLP1 and GLP2 aggregation kinetics were due to the presence of any preformed seeds, we performed electron microscopy of the peptide solutions (supernatant after ultracentrifugation) immediately after sample preparation on day 0. Our data suggested that both GLP1 and GLP2 showed mostly amorphous structure similar to monomeric and/or low molecular amyloid-β peptides.[46] Careful inspection of the electron micrographs showed that GLP2 forms relatively higher-order species compared to GLP1 (Figure S2). It is interesting to note that upon addition of heparin GLP1 showed a marked increase in higher-order species, whereas there was very little difference observed in the case of GLP2 with or without heparin (Figure S2).

Heparin Induces Secondary-Structure Changes in GLP1 and Accelerates Fibrillation. Far-UV circular dichroism (CD) spectropolarimetry is routinely used to monitor the secondary-structure transition and peptide/protein aggregation.[47,48] Characterization of β-sheet-rich amyloid fibrils by proteins is often indicated by a negative minimum at ~218 nm in CD spectra. Time-dependent changes in the secondary structure of the incubated GLP samples were monitored by CD. Immediately after dissolution, GLP1 was mostly unstructured in solution (Figure 2A), whereas in presence of heparin, CD spectra of GLP1 show two minima, one at 208 nm and the other at 222 nm, indicating a mostly helical conformation on day 0 (Figure 2B). The data suggests significant conformational changes of GLP1 in the presence of heparin. When GLP1 samples in the presence or absence of heparin were incubated at 37 °C, the secondary structure of GLP1 under both conditions gradually transformed to a largely β-sheet-rich structure. Interestingly, the rate of conformational transition of GLP1 in the presence of heparin was faster than that of GLP1 in the absence of heparin (Figure 2A,B). It is interesting to note that the CD negative minima intensity (at 218 nm) for GLP1 on day 30 in the presence of heparin was almost double the magnitude compared to that in the absence of heparin. This indicates an increase in β-sheet content of the resultant fibril in the presence of heparin, as was also suggested in previous studies for apomyoglobin fibrillation.[26] An alternative explanation could be that the presence of heparin changes the molecular packing structure of fibrils formed by GLP1, which is supported by differences in fibril morphology in EM (Figure 4). Previous studies also showed that sulfate ions modulate the morphology and secondary structure of glucagon fibrils.[32]

GLP2, however, showed mostly helical conformation on day 0 both in the presence and absence of heparin, which eventually became converted to a β-sheet-rich structure representing amyloid formation (Figure 2D,E). It is interesting to note that unlike GLP1, GLP2 does not show any dependence on heparin for its conformational transition kinetics.

ANS Binding Studies Show Relative Hydrophobic Surface Exposure During GLP Aggregation. During the course of amyloid formation, peptides/proteins might frequently access oligomeric states,[49] which could be either an off-pathway or on-pathway intermediate. The native

monomers and fibrillar states have less hydrophobic surface exposure, whereas oligomers have a higher hydrophobic exposure, which could be due to an increased surface-to-volume ratio of the latter.[50] The fluorescent dye 8-anilino-1-naphthalene sulfonate (ANS) has been used to probe the solvent-exposed hydrophobic surface during the process of aggregation.[51] In this study, we utilized ANS fluorescence to understand the extent of hydrophobic surface exposure during oligomerization of the GLPs. ANS fluorescence for GLP1 in the presence or absence of heparin increases and reaches its maximum value on day 7 of the incubation (Figure 3A). The
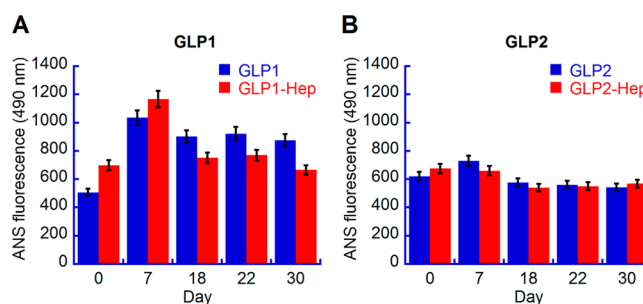

Figure 3. ANS fluorescence during GLP1 and GLP2 amyloid formation. (A) ANS fluorescence recorded for GLP1 both in the absence (GLP1) and presence of heparin (GLP1-Hep) initially showed an increase in intensity up to day 7 followed by a decline with time. This decline is more significant for GLP1-Hep than for GLP1 alone. (B) GLP2 both in the absence (GLP2) and presence of heparin (GLP2-Hep) showed a slight increase in intensity up to day 7 followed by a decline with time. Fluorescence readings were taken at the time points indicated in the figure.

ANS binding to GLP1 in the presence of heparin was slightly higher compared to that of GLP1 alone, indicating high hydrophobic surface exposure because of faster initial oligomerization of GLP1 in the presence of heparin. After day 7, a decline in ANS fluorescence was observed in both cases (Figure 3A) during fibril formation. However, the extent of the decline for GLP1-Hep was more prominent than for GLP1 without heparin, indicating faster fibrillation of GLP1 in the presence of heparin. At the end of fibrillation, GLP1 showed more ANS binding compared to GLP1-Hep fibrils, suggesting that more compact and less hydrophobic surface-exposed fibrils were formed by GLP1 in the presence of heparin. However, GLP2 in the absence or presence of heparin showed a slight increase in ANS fluorescence intensity up to day 7 followed by a constant decrease in ANS fluorescence with successive periods of incubation (Figure 3B), suggesting that heparin probably does not play an important role in GLP2 fibrillation. The magnitudes of ANS binding to GLP2 in the presence and absence of heparin during the entire period of aggregation were much lower (except for day 0 without heparin) compared to GLP1. This indicates lesser hydrophobic surface exposure throughout the duration of aggregation for GLP2.

Electron Microscopy Showed Amyloid-Like Aggregates of Peptides. Transmission electron microscopy was done to visualize the morphology of the 30 day-incubated GLP samples. All four samples (GLP1, GLP1-Hep, GLP2, and GLP2-Hep) showed fibrillar morphology by electron microscopy, indicating the formation of amyloid fibrils (Figure 4). These fibrils were composed of ~2−4 individual filaments. GLP1 showed a mixture of wavy and straight fibrils, whereas GLP1-Hep and GLP2 showed predominantly short and straight
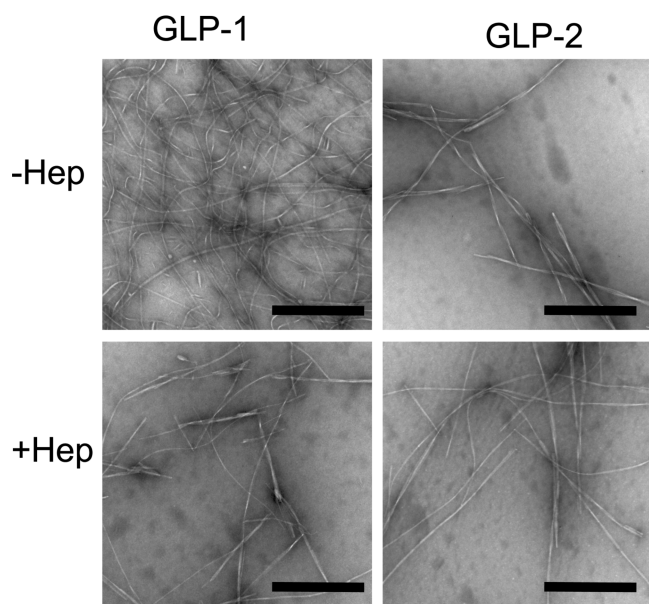
GLP-1   GLP-2

-Hep

+Hep

Figure 4. Electron microscopic images of GLP amyloid fibrils formed in the presence or absence of heparin. The scale bar is 500 nm.

Figure 5. Tryptophan fluorescence and acrylamide quenching assay. Trp fluorescence before and after fibril formation of GLP1 (A) and GLP2 (B) in the presence or absence of heparin. Stern−Volmer plot of GLP1 (C) shows a change in slope in the presence or absence of heparin because of Trp internalization (A, blue shift), whereas GLP2 (D, in the absence or presence of heparin) does not show any marked change.

fibrils. GLP2-Hep, however, showed slightly longer fibrils, with some displaying a curved nature. Because GLP2 with or without heparin showed identical amyloid formation kinetics and a similar fibril morphology, we analyzed GLP2 (with or without heparin) at different time points starting from day 0 until the state of amyloid formation using TEM. The results indicate that the fibril growth was alike for GLP2 under both conditions (Figure S3).

Relative Solvent Exposure of Tryptophan Is Altered in GLP1 during Aggregation. Tryptophan (Trp) is routinely used for intrinsic fluorescence measurements in protein/peptide folding and aggregation. During protein folding or aggregation, tryptophan's fluorescence maximum and intensity depend on its local environment within the peptide.[52] To examine whether amyloid formation is accompanied by changes in Trp microenvironments, we utilized the single Trp residue present in the C-terminus of the GLPs to study their intrinsic fluorescence. Trp fluorescence was performed at the beginning (d0) and at the end of amyloid formation (d30) for both GLPs.

GLP1 showed fluorescence intensity maxima (∼3000 FU) around 350 nm, suggesting that Trp is mostly solvent-exposed on day 0. In the presence of heparin, GLP1 showed almost double the fluorescence intensity (∼7000 FU) with fluorescence intensity maxima at 350 nm, suggesting a different Trp microenvironment (Figure 5A, d0). After fibril formation (Figure 5A, d30), Trp in GLP1 showed an increase in fluorescence intensity (∼5000 FU) with a blue-shifted fluorescence maxima at ∼335 nm. This indicates that Trp is less solvent-exposed and in a more hydrophobic environment in the fibrillar state. Similarly, GLP1-Hep fibrils showed a drastic increase in fluorescence intensity (∼10 000 FU) with a blue-shifted fluorescence intensity maxima at ∼330 nm, suggesting that GLP1-Hep fibrils are more compact and that Trp is in a more hydrophobic core compared to GLP1 fibrils alone. Trp fluorescence of GLP2 with or without heparin showed a fluorescence intensity of ∼4500 FU at 350 nm, suggesting that Trp is solvent-exposed in its nonaggregated state (d0) (Figure 5B). After incubation, both in the presence and absence of heparin, GLP2 fluorescence intensity was
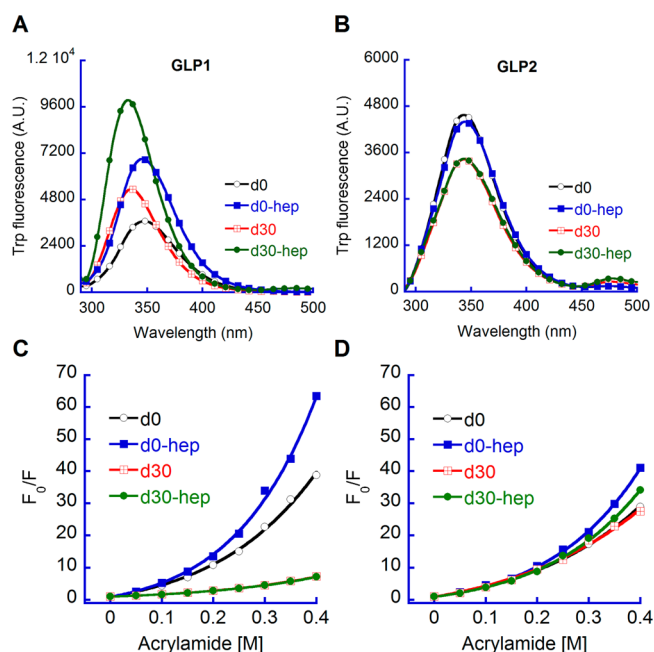
slightly decreased (∼3500 FU). However, there was no change in the λ_{max} value of either the nonaggregated (d0) or amyloid state (d30), implying that the Trp site of GLP2 did not undergo major structural conversion during fibril formation. We carried out acrylamide quenching to delineate further the relative solvent exposure of tryptophan residue for both GLPs on day 0 and after amyloid formation. The ratio (F_0/F) of fluorescence intensity in the absence (F_0) and presence (F) of quencher was plotted against quencher concentration $[Q]$, and the slope of the curve was analyzed using a modified Stern−Volmer equation. Acrylamide quenching of GLP1 in the absence or presence of heparin showed a decrease in slope on day 30 (smaller K_{sv} value) in comparison to day 0 (Figure 5C and Table S1). However, GLP2 in the presence and absence of heparin also showed a decrease in K_{sv} because of fibril formation, although the extent of the change was much less compared to GLP1 (Figure 5D and Table S1). These results indicate that during the course of aggregation the tryptophan residue of GLP1 became buried, whereas in the case of GLP2, there was very little change in the microenvironment of tryptophan.

Heparin Preferentially Interacts with GLP1 and Increases Its Fibril Intactness. Heparin has been reported to play an important role in the aggregation of proteins associated with various functions and diseases,[19,53] wherein it acts as a catalyst at the early stage of fibril formation, promoting nucleation and increased fibrillation.[53] Heparin is proposed to serve as a scaffold that increases the local concentration of monomers and allows faster fibril formation, wherein it gets integrated into the fibril structure.[54] We carried out dot-blot analysis of GLP1-Hep and GLP2-Hep fibrils using an anti-heparin antibody to determine if heparin is bound to these amyloid fibrils. It was interesting to observe a relatively

increased binding (signal intensity) of the antibody to the GLP1-Hep fibrils relative to the GLP2-Hep fibrils (Figure 6A),
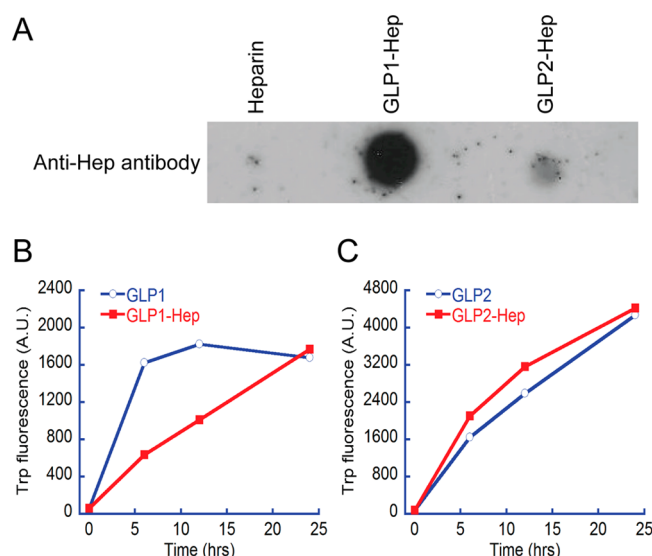

Figure 6. (A) Dot blot of GLP1 and GLP2 amyloid fibrils formed in the presence of heparin. Equal concentrations of GLP1-Hep and GLP2-Hep fibrils and heparin alone were spotted and probed with an anti-heparin antibody. The intense signal for the GLP1-Hep sample shows increased association of heparin with GLP1 fibrils. A possible reason for the absence of any signal on heparin alone spotted region (left most) could be due to weak binding/lack of binding of heparin to the membrane, which was removed during the washing steps. (B, C) Monomer release assay. At regular time intervals during the release assay, the peptide monomers released outside the membrane were monitored by Trp fluorescence. GLP1 fibrils formed in the absence of heparin appear to release the monomers at a faster rate when compared to GLP1 fibrils formed in the presence of heparin (B). Such an effect of heparin is not apparent in the case of GLP2, where the monomer release profiles are quite similar in the absence or presence of heparin (C).

suggesting that heparin becomes integrated to a greater extent into the GLP1 fibrils as opposed to the GLP2 fibrils. We propose that integration of heparin within the GLP1 fibrils could possibly play a role in enhancing the fibril stability or intactness. To affirm this, we examined monomer release potency of the GLP amyloids formed in the presence or absence of heparin. GLP amyloid fibrils release their monomer counterparts with time when subjected to a release assay. The extent of monomer release was assessed by Trp fluorescence in the outer solution (solution outside the dialysis membrane). Although the rate of monomer release differed significantly for GLP1 in the presence or absence of heparin (Figure 6B), there was no apparent variation in the case of GLP2 under similar conditions (Figure 6C). In the case of the GLP1 fibrils that formed in the absence of heparin, a drastic increase in Trp fluorescence was observed, indicating that an increased amount of monomers was released outside the membrane (Figure 6B). The monomer release reached saturation after 6 h and remained stationary thereafter until the end of the study (24 h). However, GLP1-Hep fibrils showed a gradual increase in Trp fluorescence with time (Figure 6B), indicating the role of heparin in increasing GLP1 fibril stability, allowing a slow release of monomeric GLP1 from the fibrils. However, the monomer release profile of GLP2 fibrils formed in the presence or absence of heparin was similar (Figure 6C). Unlike GLP1

(without heparin), there was no spontaneous release observed in GLP2 or GLP2-Hep, instead there was a gradual Trp fluorescence increase with time in both of these cases. These results indicate the potential role of heparin in preferentially stabilizing GLP1 fibrils over GLP2 fibrils.

GLP1 and GLP2 Show Distinct Heparin-Binding Potencies in Silico. All-atom molecular dynamics simulation (MD) is a powerful tool for the estimation of bonding patterns and stability of macromolecular interactions. MD simulations have previously been used to study biological phenomenon like protein folding and protein aggregation in silico.[12,55−58]

Owing to the differential interaction of heparin with GLP1 and GLP2 in vitro, we further probed the two peptides for their interactions with heparin using all-atom molecular dynamics simulations. The results of the MD simulations support the experimental findings, which suggest that heparin promotes GLP1 aggregation, whereas it does not seem to affect GLP2 aggregation. The 100 ns simulation of GLP1 reveals the dense clustering of the peptides around the heparin backbone at the end of the simulation time (Figure 7A, top, 100 ns). In contrast, heparin does not seem to have an influence on GLP2 aggregation (Figure 7A, bottom, 100 ns). Figure S4 illustrates the manner in which the GLP1 peptides cluster together and aggregate around the glycosaminoglycan as time progresses, eventually forming a denser network around it (Figure S4, top panel). GLP2 peptides, however, self-associated into an aggregated cluster away from the heparin backbone (Figure S4, bottom panel).

The interpeptide hydrogen bonding of the two peptides showed a similar trend during the simulation (Figure 7B, left). Interestingly and consistent with our in vitro data, the peptide−heparin interaction was markedly different in GLP1 as compared to GLP2, with the former displaying increased H-bonding with heparin during the simulation (Figure 7B, right). GLP2, however, exhibits very little change in H-bonding with heparin throughout the simulation (Figure 7B, right). To probe the preferential interaction of heparin with GLP1 during aggregation over GLP2, we further investigated the amino acids that interacted with the heparin during the simulation. Although the residues involved in the interaction of GLP1 and GLP2 with heparin were predominantly basic (positively charged) in nature, the close proximity of the basic residues in the primary structure of GLP1 seems to play a crucial role in its binding to heparin. The extent of involvement of different amino acid residues in the GLP1−heparin interaction is shown in Figure 7C. We observed that three out of the four GLP1 peptides (P1, P2, P4, and P7) interacting with heparin overwhelmingly displayed H-bonding between side chains of alternating basic residues (K28 and R30) with heparin (Figure 7C, left). Despite the presence of charged interacting residues (H1 and R20) in GLP2 (Figure 1), their separation in the primary structure might be the causative factor for the lower heparin interaction (Figure 7C, right). These findings are further substantiated by the orientation of interacting residues of GLP1 and GLP2 with the heparin backbone, as represented in Figure 8. The close orientation of the charged residues (LYS28 and ARG30) on heparin demonstrates their role in stabilizing heparin−peptide interactions (Figure 8A). The LIGPLOT 2D interaction map of GLP1 and GLP2 with heparin shows that the GLP1−heparin interaction is much denser as compared to the GLP2−heparin profile (Figure S5). The map also establishes the possible reason for the strength of the GLP1−heparin complex, which shows numerous hydro-
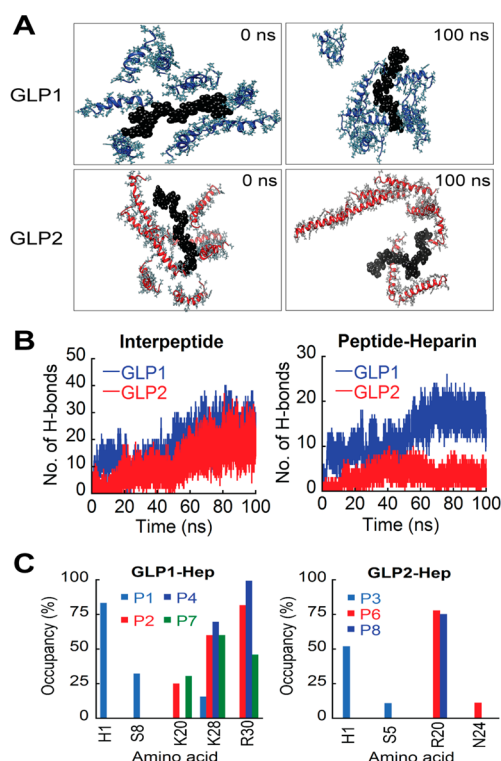
Figure 7. Molecular dynamics Simulations of GLP1 and GLP2. (A) Left panel shows the initial state of the system (t = 0 ns), whereas the right panel indicates the final state (t = 100 ns). The GLP1 peptide system on the top-right shows the nature of the heparin incorporated aggregate, whereas the GLP2 aggregates shown in the bottom-right do not involve heparin. (B) Interpeptide H-bonding (left panel) in GLP1 and GLP2 shows a tendency to increase with time. The peptide—heparin interaction shows an increasing trend in the GLP1 system, whereas the GLP2—heparin interaction shows very little change throughout the simulation. (C) Positively charged residues (K28 and R30) along with H1 of GLP1 show a high H-bonding frequency with heparin side chains (left panel). The GLP1 peptides P1, P2, P4, and P7 in the simulation system most frequently interacted with heparin. The right panel shows the interacting residues from GLP2 peptides (P3, P6, and P8) in the simulation system. The charged R20 residue is seen to be involved in interaction with heparin in two out of the three interacting peptides.

phobic interactions in addition to hydrogen-bonded interactions. GLP2, however, does not seem to exhibit any such propensity (Figure S5, right).

DISCUSSION

Studying the effect of GAGs on protein aggregation and amyloid formation is important because GAGs have been shown to play a significant role not only in disease-related amyloid formation[17−24] but also in the formation of amyloid-like structures in secretory granules.[4] It has been previously reported that heparin, a representative GAG, reduces the toxicity of Aβ fibrils associated with Alzheimer's disease.[59] It was suggested by different groups that the charged interactions between protein and GAGs could play a crucial role in modulating protein/peptide amyloid formation[22,60,61] as well as its stability.[62,63] For example, positively charged residues in protein and negatively charged sulfate ions in heparin have been suggested to interact, which increases the local concentration of protein/peptide and leads to their fibrillation.[27,64] However, the detailed mechanism of protein—heparin
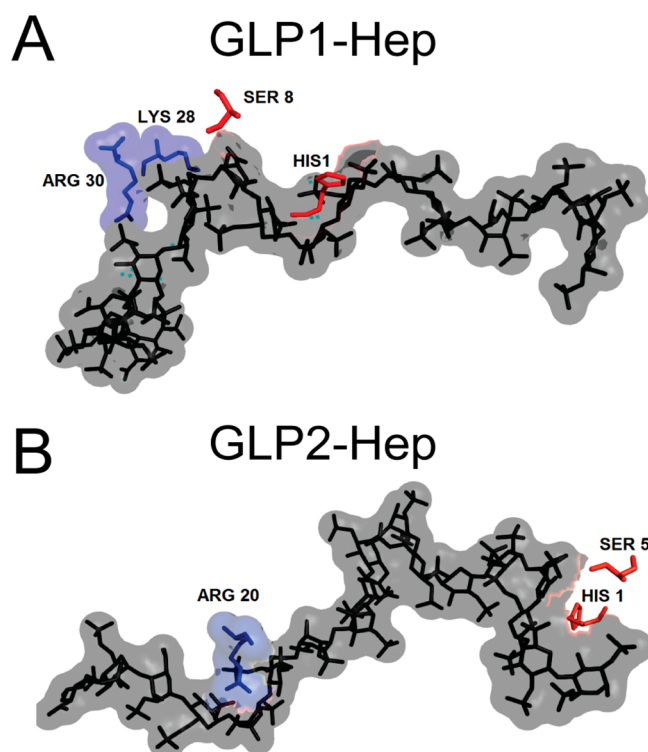

Figure 8. Three-dimensional interaction profile of GLP1 and GLP2 with Heparin. (A) Three-dimensional interaction profile of GLP1 and heparin (black surface) with the highest-frequency interaction residues, Lys28 and Arg30, shown in blue, and the other interacting residues, His1 and Ser8, shown in red. (B) Three-dimensional interaction map of GLP2 and heparin showing the highest-frequency residue Arg20 (blue surface) closely interacting with heparin. The images were rendered using PyMol. (Note that Lys28 and Arg30 in GLP1 (7−37) from PDB corresponds to Lys34 and Arg36, respectively, in GLP1 (1−37).)

interaction and the requirement of any specific positioning of positively charged residues in protein/peptides for heparin interactions are not yet clear. In our study, we used two peptides, GLP1 and GLP2, that have a number of similarities: both possess a helix-rich conformation and a similar distribution of hydrophobic and hydrophilic residue positioning (Figure 1, sequence homology), and both are highly amyloidogenic as predicted by the TANGO algorithm[65] and demonstrated by previous studies.[4,66] However, our biophysical data showed that the kinetics of amyloid formation by these two peptides is strikingly different. Fibrillation of GLP1 followed a nucleation-dependent polymerization mechanism with a distinct lag time, elongation, and stationary phase. This fibril formation involved a large structural transition of α-helix → β-sheet, as was evident from the CD data. The lag time, however, was significantly reduced when heparin was added to the reaction mixture, suggesting that heparin—GLP1 interaction increased the local concentration of GLP1, resulting in faster fibrillation (Figure 2C). In contrast, although GLP2 is also involved in an α-helix → β-sheet transition during fibril formation, it exhibits a very short lag time during amyloid formation. Thus, it is possible that GLP2 started with a structural state that was favorable for aggregation (fibril-competent) from the beginning of the reaction (Figure S2). This allows the reaction to proceed more favorably to the exponential phase, circumventing any significant lag time

(Figure 2F). Moreover, the addition of heparin did not significantly alter the kinetics of GLP2 fibrillation, suggesting that this peptide may not strongly interact with heparin. We hypothesize that monomeric or oligomeric species of GLP2 (in the absence or presence of heparin) with high exposed hydrophobic surface (high ANS binding, Figure 3B) most likely populate the fibril-competent state at the beginning of the aggregation itself. Indeed, GLP1 shows relatively low ANS binding at the beginning compared to GLP2 and increases later to peak at an intermediate time point. Further, ANS binding decreases as higher-order structures with shielded hydrophobic surfaces begin to form. Our speculation that GLP2 aggregation starts with a fibril-competent structure is further corroborated by the fact that Trp[25], located in the amyloidogenic region (amino acids 22−27, Figure S1), did not show any major site-specific structural changes (Figure 5, Trp fluorescence and acrylamide quenching) before and after aggregation. A similar observation was also obtained for GLP2 in the presence of heparin. In contrast, Trp[31], present in the amyloidogenic region of GLP1 (amino acids 28−34, Figure S1), showed a drastic change in its microenvironment when transitioning from a soluble to a fibrillar form. The dot blot and monomer release of GLP fibrils suggest that heparin not only modulates GLP1 fibrillation but also gets incorporated into GLP1 fibrils, resulting in slow monomer release upon dialysis. In contrast, heparin neither gets incorporated into GLP2 fibrils nor does it significantly affect the monomer release profile.

The differential effect of heparin on GLP1 and GLP2 fibrillation could be due to two reasons: (1) primary sequences with different positioning of basic amino acids in the peptides or (2) accessibility of heparin to its binding sites on the peptides. If heparin were to function as a scaffold where monomers could bind/attach and further nucleate to form higher-order structures, then an adequate accessibility of the heparin interacting sites on the peptide/protein is necessary. In the present study, this assertion is true for the GLP1 peptide. In contrast, GLP2 assumes a structure to which heparin probably is not able to bind or vice versa.

The roles of anions in promoting the aggregation of several proteins[67,68] have been reported previously. Furthermore, sulfate ions have been suggested to influence fibrillation of amyloidogenic proteins, including $A\beta$ and transthyretin (TTR).[62,69] More importantly, amyloid formation of a closely related peptide-hormone glucagon seems to be greatly influenced by the presence of sulfate ions.[32] The plausible explanation for this is the interaction of the negatively charged sulfate groups with the positively charged residues in the primary sequence of the protein. In addition, recent reports suggests that sulfated glycosaminoglycan heparin binds to positively charged amino acid residues, especially when they are present in an alternating fashion (basic-nonbasic-basic) in a protein.[25−28] There are four positively charged amino acid residues in GLP1, two of which are present at the C-terminal region in an alternating manner (residues 34−36; KGR). Heparin might interact with these basic residues and act as a template for nucleation and subsequent fibrillation of GLP1.

Furthermore, from our MD simulation results, the KGR motif (residues 28−30 in GLP1 (7−37) structure from PDB ID 1D0R) was observed to be the common interacting region for all of the heparin interacting peptides: P1, P2, P4, and P7 (Figure 7C, left). This data implies the importance of basic-nonbasic-basic (B-X-B) motif in protein/peptides for heparin binding. GLP2, however, has only two basic residues that are far apart in the primary sequence (R20 and K30) (Figure 1A), possibly reducing the likelihood of heparin interaction with it. The MD simulation data show the strong involvement of basic residues, R20 and H1 of GLP2, in heparin interaction, but these interactions are seen in fewer peptides, further reiterating the necessary role of basic residues in close proximity (e.g., B-X-B) in stabilizing protein−heparin binding. Although basic residues throughout the sequence might be involved in stabilizing the binding of peptides to the heparin backbone, in the absence of the B-X-B motif, the more distantly spaced basic residues might not sufficiently stabilize the interaction, as seen from our simulation results (Figure 7C, right).

CONCLUSIONS

In this work, we studied the detailed mechanism of aggregation and amyloid formation by two closely related peptides, GLP1 and GLP2, in the presence and absence of heparin. Our biophysical data along with all-atom MD simulations suggest the differential effect of heparin on GLP1 and GLP2 aggregation and amyloid formation. This study not only signifies the role of glycosaminoglycans in amyloid formation of protein/peptides targeted to the regulatory secretory pathway in mammalian cells but also reveals the precise nature of the peptide−heparin interaction. Furthermore, atomistic MD simulations indicate the stable nature of the charge interactions between GLP1 and heparin that promote the increase in the local concentration around the GAG backbone, thereby driving aggregation. Thus, we emphasize that the presence of basic residues in close proximity in the amino acid sequence of peptides/proteins is a key feature of heparin-mediated aggregation. Our study will significantly help to understand the mechanism(s) of GLP1 and GLP2 aggregation and amyloid formation relevant to their storage inside secretory granules.

ASSOCIATED CONTENT

Ⓢ Supporting Information

Detailed information on the predicted aggregation profile of the GLP1 and GLP2 peptides, electron micrograph images of the GLP1 and GLP2 (in the presence and absence of heparin) on day 0, electron micrograph images of the GLP2 (in the presence and absence of heparin) at various time points during the course of amyloid formation, time progression of the two systems during the MD simulation, detailed interaction map of GLP1 and GLP2 with heparin, and Stern−Volmer constants (K_{sv}) for acrylamide quenching of glucagon-like peptides before and after amyloid formation. This material is available free of charge via the Internet at http://pubs.acs.org.

AUTHOR INFORMATION

Corresponding Author

*Telephone: +91-22-2576-7774. Fax: +91-22-2572-3480. E-mail: samirmaji@iitb.ac.in.

Author Contributions

[†]These authors contributed equally to this work. All authors designed the experiments and analyzed the data, and all authors except for S.K.M. and R.P. carried out the experiments. All authors participated in writing the manuscript. The final version of the manuscript has been approved by all authors.

■ ABBREVIATIONS USED

ANS, 8-anilino-1-naphthalenesulfonic acid; CD, circular dichroism; D-man, D-mannitol; GAGs, glycosaminoglycans; GLP1, glucagon-like peptide-1; GLP2, glucagon-like peptide-2; Hep, heparin; MD, molecular dynamics; PBST, phosphate buffered saline with tween 20; PDB, Protein Data Bank; TBST, tris buffered saline with tween 20; TEM, transmission electron microscopy; ThT, thioflavin T; Trp, tryptophan; UV, ultraviolet

■ REFERENCES

(1) Chiti, F., and Dobson, C. M. (2006) Protein misfolding, functional amyloid, and human disease. *Annu. Rev. Biochem. 7S*, 333−366.

(2) Fowler, D. M., Koulov, A. V., Balch, W. E., and Kelly, J. W. (2007) Functional amyloid−from bacteria to humans. *Trends Biochem. Sci. 32*, 217−224.

(3) Fowler, D. M., Koulov, A. V., Alory-Jost, C., Marks, M. S., Balch, W. E., and Kelly, J. W. (2006) Functional amyloid formation within mammalian tissue. *PLoS Biol. 4*, e6.

(4) Maji, S. K., Perrin, M. H., Sawaya, M. R., Jessberger, S., Vadodaria, K., Rissman, R. A., Singru, P. S., Nilsson, K. P., Simon, R., Schubert, D., Eisenberg, D., Rivier, J., Sawchenko, P., Vale, W., and Riek, R. (2009) Functional amyloids as natural storage of peptide hormones in pituitary secretory granules. *Science 325*, 328−332.

(5) Kelly, R. B. (1985) Pathways of protein secretion in eukaryotes. *Science 230*, 25−32.

(6) Arvan, P., and Castle, D. (1998) Sorting and storage during secretory granule biogenesis: Looking backward and looking forward. *Biochem. J. 332*, 593−610.

(7) Dannies, P. S. (2001) Concentrating hormones into secretory granules: Layers of control. *Mol. Cell. Endocrinol. 177*, 87−93.

(8) Dannies, P. S. (2002) Mechanisms for storage of prolactin and growth hormone in secretory granules. *Mol. Genet. Metab. 76*, 6−13.

(9) Tooze, S. A. (1998) Biogenesis of secretory granules in the trans-Golgi network of neuroendocrine and endocrine cells. *Biochim. Biophys. Acta 1404*, 231−244.

(10) Anderson, R. G., and Pathak, R. K. (1985) Vesicles and cisternae in the trans Golgi apparatus of human fibroblasts are acidic compartments. *Cell 40*, 635−643.

(11) Jain, R. K., Joyce, P. B., and Gorr, S. U. (2000) Aggregation chaperones enhance aggregation and storage of secretory proteins in endocrine cells. *J. Biol. Chem. 275*, 27032−27036.

(12) Ranganathan, S., Singh, P. K., Singh, U., Singru, P. S., Padinhateeri, R., and Maji, S. K. (2012) Molecular interpretation of ACTH-β-endorphin coaggregation: Relevance to secretory granule biogenesis. *PLoS One 7*, e31924-1−e31924-12.

(13) Maji, S. K., and Riek, R. (2010) Formation of secretory granules involve the amyloid structure, in *Functional Amyloid Aggregation* (Rigacci, S., and Bucciantini, M., Eds.) pp 135−155, Research Signpost, Kerala, India.

(14) Kolset, S. O., Prydz, K., and Pejler, G. (2004) Intracellular proteoglycans. *Biochem. J. 379*, 217−227.

(15) Reggio, H. A., and Palade, G. E. (1978) Sulfated compounds in the zymogen granules of the guinea pig pancreas. *J. Cell Biol. 77*, 288−314.

(16) Carlson, S. S., and Kelly, R. B. (1983) A highly antigenic proteoglycan-like component of cholinergic synaptic vesicles. *J. Biol. Chem. 258*, 11082−11091.

(17) Su, J. H., Cummings, B. J., and Cotman, C. W. (1992) Localization of heparan sulfate glycosaminoglycan and proteoglycan core protein in aged brain and Alzheimer's disease. *Neuroscience 51*, 801−813.

(18) Cohlberg, J. A., Li, J., Uversky, V. N., and Fink, A. L. (2002) Heparin and other glycosaminoglycans stimulate the formation of amyloid fibrils from alpha-synuclein in vitro. *Biochemistry 41*, 1502−1511.

(19) Snow, A. D., Kisilevsky, R., Willmer, J., Prusiner, S. B., and DeArmond, S. J. (1989) Sulfated glycosaminoglycans in amyloid plaques of prion diseases. *Acta Neuropathol. 77*, 337−342.

(20) Athanasou, N. A., West, L., Sallie, B., and Puddle, B. (1995) Localized amyloid deposition in cartilage is glycosaminoglycans-associated. *Histopathology 26*, 267−272.

(21) Athanasou, N. A., Kokubun, S., West, L., Sallie, B., and Puddle, B. (1995) Glycosaminoglycans in intervertebral disc amyloid deposits. *Eur. Spine J. 4*, 308−312.

(22) Valle-Delgado, J. J., Alfonso-Prieto, M., de Groot, N. S., Ventura, S., Samitier, J., Rovira, C., and Fernandez-Busquets, X. (2010) Modulation of Aβ42 fibrillogenesis by glycosaminoglycan structure. *FASEB J. 24*, 4250−4261.

(23) Suk, J. Y., Zhang, F., Balch, W. E., Linhardt, R. J., and Kelly, J. W. (2006) Heparin accelerates gelsolin amyloidogenesis. *Biochemistry 45*, 2234−2242.

(24) Bourgault, S., Solomon, J. P., Reixach, N., and Kelly, J. W. (2011) Sulfated glycosaminoglycans accelerate transthyretin amyloidogenesis by quaternary structural conversion. *Biochemistry 50*, 1001−1015.

(25) Cardin, A. D., and Weintraub, H. J. (1989) Molecular modeling of protein-glycosaminoglycan interactions. *Arteriosclerosis 9*, 21−32.

(26) Vilasi, S., Sarcina, R., Maritato, R., De Simone, A., Irace, G., and Sirangelo, I. (2011) Heparin induces harmless fibril formation in amyloidogenic W7FW14F apomyoglobin and amyloid aggregation in wild-type protein in vitro. *PLoS One 6*, e22076-1−e22076-13.

(27) Noborn, F., O'Callaghan, P., Hermansson, E., Zhang, X., Ancsin, J. B., Damas, A. M., Dacklin, I., Presto, J., Johansson, J., Saraiva, M. J., Lundgren, E., Kisilevsky, R., Westermark, P., and Li, J. P. (2011) Heparan sulfate/heparin promotes transthyretin fibrillization through selective binding to a basic motif in the protein. *Proc. Natl. Acad. Sci. U.S.A. 108*, 5584−5589.

(28) Fowlkes, J. L., Thrailkill, K. M., George-Nascimento, C., Rosenberg, C. K., and Serra, D. M. (1997) Heparin-binding, highly basic regions within the thyroglobulin type-1 repeat of insulin-like growth factor (IGF)-binding proteins (IGFBPs) -3, -5, and -6 inhibit IGFBP-4 degradation. *Endocrinology 138*, 2280−2285.

(29) Ghodke, S., Nielsen, S. B., Christiansen, G., Hjuler, H. A., Flink, J., and Otzen, D. (2012) Mapping out the multistage fibrillation of glucagon. *FEBS J. 279*, 752−765.

(30) Andersen, C. B., Hicks, M. R., Vetri, V., Vandahl, B., Rahbek-Nielsen, H., Thogersen, H., Thogersen, I. B., Enghild, J. J., Serpell, L. C., Rischel, C., and Otzen, D. E. (2010) Glucagon fibril polymorphism reflects differences in protofilament backbone structure. *J. Mol. Biol. 397*, 932−946.

(31) Andersen, C. B., Otzen, D., Christiansen, G., and Rischel, C. (2007) Glucagon amyloid-like fibril morphology is selected via morphology-dependent growth inhibition. *Biochemistry 46*, 7314−7324.

(32) Pedersen, J. S., Flink, J. M., Dikov, D., and Otzen, D. E. (2006) Sulfates dramatically stabilize a salt-dependent type of glucagon fibrils. *Biophys. J. 90*, 4181−4194.

(33) Mojsov, S., Heinrich, G., Wilson, I. B., Ravazzola, M., Orci, L., and Habener, J. F. (1986) Preproglucagon gene expression in pancreas

and intestine diversifies at the level of post-translational processing. *J. Biol. Chem. 261*, 11880−11889.

(34) Kieffer, T. J., and Habener, J. F. (1999) The glucagon-like peptides. *Endocr. Rev. 20*, 876−913.

(35) Phillips, J. C., Braun, R., Wang, W., Gumbart, J., Tajkhorshid, E., Villa, E., Chipot, C., Skeel, R. D., Kale, L., and Schulten, K. (2005) Scalable molecular dynamics with NAMD. *J. Comput. Chem. 26*, 1781−1802.

(36) Willander, H., Presto, J., Askarieh, G., Biverstal, H., Frohm, B., Knight, S. D., Johansson, J., and Linse, S. (2012) BRICHOS domains efficiently delay fibrillation of amyloid beta-peptide. *J. Biol. Chem. 287*, 31608−31617.

(37) (2010) *The PyMOL Molecular Graphics System, Version 1.3r1*, Schrödinger, LLC, Porland, OR.

(38) Pettersen, E. F., Goddard, T. D., Huang, C. C., Couch, G. S., Greenblatt, D. M., Meng, E. C., and Ferrin, T. E. (2004) UCSF Chimera—a visualization system for exploratory research and analysis. *J. Comput. Chem. 25*, 1605−1612.

(39) Wallace, A. C., Laskowski, R. A., and Thornton, J. M. (1995) LIGPLOT: A program to generate schematic diagrams of protein-ligand interactions. *Protein Eng. 8*, 127−134.

(40) Biancalana, M., Makabe, K., Koide, A., and Koide, S. (2009) Molecular mechanism of thioflavin-T binding to the surface of beta-rich peptide self-assemblies. *J. Mol. Biol. 385*, 1052−1063.

(41) Ban, T., Hamada, D., Hasegawa, K., Naiki, H., and Goto, Y. (2003) Direct observation of amyloid fibril growth monitored by thioflavin T fluorescence. *J. Biol. Chem. 278*, 16462−16465.

(42) Ferrone, F. (1999) Analysis of protein aggregation kinetics. *Methods Enzymol 309*, 256−274.

(43) Naiki, H., Higuchi, K., Nakakuki, K., and Takeda, T. (1991) Kinetic analysis of amyloid fibril polymerization in vitro. *Lab. Invest. 65*, 104−110.

(44) Pedersen, J. S., and Otzen, D. E. (2008) Amyloid − a state in many guises: Survival of the fittest fibril fold. *Protein Sci. 17*, 2−10.

(45) LeVine, H., 3rd (1993) Thioflavine T interaction with synthetic Alzheimer's disease β-amyloid peptides: Detection of amyloid aggregation in solution. *Protein Sci. 2*, 404−410.

(46) Maji, S. K., Ogorzalek Loo, R. R., Inayathullah, M., Spring, S. M., Vollers, S. S., Condron, M. M., Bitan, G., Loo, J. A., and Teplow, D. B. (2009) Amino acid position-specific contributions to amyloid β-protein oligomerization. *J. Biol. Chem. 284*, 23580−23591.

(47) Brahms, S., and Brahms, J. (1980) Determination of protein secondary structure in solution by vacuum ultraviolet circular dichroism. *J. Mol. Biol. 138*, 149−178.

(48) McCubbin, W. D., Kay, C. M., Narindrasorasak, S., and Kisilevsky, R. (1988) Circular-dichroism studies on two murine serum amyloid A proteins. *Biochem. J. 256*, 775−783.

(49) Kaylor, J., Bodner, N., Edridge, S., Yamin, G., Hong, D. P., and Fink, A. L. (2005) Characterization of oligomeric intermediates in alpha-synuclein fibrillation: FRET studies of Y125W/Y133F/Y136F α-synuclein. *J. Mol. Biol. 353*, 357−372.

(50) Cheon, M., Chang, I., Mohanty, S., Luheshi, L. M., Dobson, C. M., Vendruscolo, M., and Favrin, G. (2007) Structural reorganisation and potential toxicity of oligomeric species formed during the assembly of amyloid fibrils. *PLoS Comput. Biol. 3*, 1727−1738.

(51) Khurana, R., Gillespie, J. R., Talapatra, A., Minert, L. J., Ionescu-Zanetti, C., Millett, I., and Fink, A. L. (2001) Partially folded intermediates as critical precursors of light chain amyloid fibrils and amorphous aggregates. *Biochemistry 40*, 3525−3535.

(52) Lakowicz, J. R. (2006) Protein fluorescence, in *Principles of Fluorescence Spectroscopy*, 3rd ed., pp 529−575, Springer, New York.

(53) McLaurin, J., Franklin, T., Zhang, X., Deng, J., and Fraser, P. E. (1999) Interactions of Alzheimer amyloid-β peptides with glycosaminoglycans effects on fibril nucleation and growth. *Eur. J. Biochem. 266*, 1101−1110.

(54) Motamedi-Shad, N., Monsellier, E., and Chiti, F. (2009) Amyloid formation by the model protein muscle acylphosphatase is accelerated by heparin and heparan sulphate through a scaffolding-based mechanism. *J. Biochem. 146*, 805−814.

(55) Klimov, D. K., and Thirumalai, D. (2003) Dissecting the assembly of Aβ16−22 amyloid peptides into antiparallel beta sheets. *Structure 11*, 295−307.

(56) Cruz, L., Urbanc, B., Borreguero, J. M., Lazo, N. D., Teplow, D. B., and Stanley, H. E. (2005) Solvent and mutation effects on the nucleation of amyloid β-protein folding. *Proc. Natl. Acad. Sci. U.S.A. 102*, 18258−18263.

(57) Urbanc, B., Cruz, L., Yun, S., Buldyrev, S. V., Bitan, G., Teplow, D. B., and Stanley, H. E. (2004) In silico study of amyloid β-protein folding and oligomerization. *Proc. Natl. Acad. Sci. U.S.A. 101*, 17345−17350.

(58) Ma, B., and Nussinov, R. (2006) Simulations as analytical tools to understand protein aggregation and predict amyloid conformation. *Curr. Opin. Chem. Biol. 10*, 445−452.

(59) Timmer, N. M., Schirris, T. J., Bruinsma, I. B., Otte-Holler, I., van Kuppevelt, T. H., de Waal, R. M., and Verbeek, M. M. (2010) Aggregation and cytotoxic properties towards cultured cerebrovascular cells of Dutch-mutated Aβ40 (DAβ(1−40)) are modulated by sulfate moieties of heparin. *Neurosci. Res. 66*, 380−389.

(60) Diaz-Nido, J., Wandosell, F., and Avila, J. (2002) Glycosaminoglycans and β-amyloid, prion and tau peptides in neurodegenerative diseases. *Peptides 23*, 1323−1332.

(61) McLaurin, J., and Fraser, P. E. (2000) Effect of amino-acid substitutions on Alzheimer's amyloid-β peptide-glycosaminoglycan interactions. *Eur. J. Biochem. 267*, 6353−6361.

(62) Fraser, P. E., Nguyen, J. T., Chin, D. T., and Kirschner, D. A. (1992) Effects of sulfate ions on Alzheimer β/A4 peptide assemblies: Implications for amyloid fibril-proteoglycan interactions. *J. Neurochem. 59*, 1531−1540.

(63) Yamaguchi, I., Suda, H., Tsuzuike, N., Seto, K., Seki, M., Yamaguchi, Y., Hasegawa, K., Takahashi, N., Yamamoto, S., Gejyo, F., and Naiki, H. (2003) Glycosaminoglycan and proteoglycan inhibit the depolymerization of β2-microglobulin amyloid fibrils in vitro. *Kidney Int. 64*, 1080−1088.

(64) Castillo, G. M., Lukito, W., Wight, T. N., and Snow, A. D. (1999) The sulfate moieties of glycosaminoglycans are critical for the enhancement of β-amyloid protein fibril formation. *J. Neurochem. 72*, 1681−1687.

(65) Fernandez-Escamilla, A. M., Rousseau, F., Schymkowitz, J., and Serrano, L. (2004) Prediction of sequence-dependent and mutational effects on the aggregation of peptides and proteins. *Nat. Biotechnol. 22*, 1302−1306.

(66) Poon, S., Birkett, N. R., Fowler, S. B., Luisi, B. F., Dobson, C. M., and Zurdo, J. (2009) Amyloidogenicity and aggregate cytotoxicity of human glucagon-like peptide-1 (hGLP-1). *Protein Pept. Lett. 16*, 1548−1556.

(67) Wong, S., and Kisilevsky, R. (1990) Influence of sulphate ions on the structure of AA amyloid fibrils. *Scand. J. Immunol. 32*, 225−232.

(68) Snow, A. D., Willmer, J., and Kisilevsky, R. (1987) Sulfated glycosaminoglycans: A common constituent of all amyloids? *Lab. Invest. 56*, 120−123.

(69) Bonifacio, M. J., Sakaki, Y., and Saraiva, M. J. (1996) 'In vitro' amyloid fibril formation from transthyretin: The influence of ions and the amyloidogenicity of TTR variants. *Biochim. Biophys. Acta 1316*, 35−42.